

## Supporting Information

### **Lung Metastasis-Targeted Donut-Shaped Nanostructures Shuttled by the Margination Effect for PolyDox Generation-Mediated Penetrative Delivery into Deep Tumors**

*Min-Ren Chiang, Yu-Lin Su, Chih-Yi Chang, Chein-Wen Chang, Shang-Hsiu Hu\**

Department of Biomedical Engineering and Environmental Sciences, National Tsing Hua University, Hsinchu, 300 (Taiwan)

*E-mail: [shhu@mx.nthu.edu.tw](mailto:shhu@mx.nthu.edu.tw)*

#### **Experimental Section**

##### **Synthesis of hexagonal hematite ( $\alpha$ -Fe<sub>2</sub>O<sub>3</sub>) nanodisc and donut**

To obtain hexagonal hematite ( $\alpha$ -Fe<sub>2</sub>O<sub>3</sub>) nanodisc, 1.09 g of FeCl<sub>3</sub> · 6H<sub>2</sub>O and 2.0 mL of distilled water were dissolved in ethanol (40 mL) by magnetic stirring. When completely dissolved, 5 g of sodium acetate was added into the mixture, which was then sealed in a Teflon-lined stainless steel autoclave and maintained at 180 °C for 24 hr. After the mixture was cooled naturally to ambient temperature, the red precipitates were collected by centrifuge and washed with distilled water for three times.

To prepare the donut, 100 mg of 1-hexadecyl-trimethylammonium bromide (CTAB) in 30 mL of aqueous solution was dissolved by stirring and heating at 60 °C for 30 min with hexagonal hematite ( $\alpha$ -Fe<sub>2</sub>O<sub>3</sub>) nanodisc. After a mixture was obtained, n-octane (14.4 mL), styrene monomer (100 mg/mL), lysine (0.146mmol), tetraethyl orthosilicate (TEOS, 4.7 mmol), and 2,2'-azobis(2-methylpropionamidine) dihydrochloride (AIBA, 0.133mmol) were subsequently added to the above solution. Octane was added the mixed solution with the octane/water mass ratios 0.34. The mass ratio of H<sub>2</sub>O/TEOS/ lysine/CTAB was maintained at 300:10:0.22:1. The reaction was allowed to proceed for 4 hr at 60 °C. Then, the heating was stopped and the suspension was cooled naturally to room temperature. The cooled suspension was purified with ethanol by centrifugation 8,000 rpm for 15 min.

The suspension was washed twice with ethanol. Finally, the template was completely removed by calcination at 500 °C for 3 hr under N<sub>2</sub>. Other particles such as sphere and ellipse were prepared with similar process with various concentrations of reagents shown in Table S1.

### **Modification of PGA with hydrazide groups and pDox fabrication**

The functionalization of poly ( $\gamma$ -glutamic acid) (PGA) with hydrazine groups was carried out in aqueous conditions. In brief, PGA was dissolved in distilled water to obtain a 0.6 wt% solution and then reacted with adipic acid dihydrazide (ADH) in the presence of 1-ethyl-3-(3-(dimethylaminopropyl) carbodiimide hydrochloride (EDC) and hydroxybenzotriazole (HOBt). The molar ratio of –COOH of PGA to ADH was set at 1:6, and EDC to HOBt was 1:1. While the molar ratio of EDC to –COOH of PGA was 1:1, 2:1, 3:1, respectively. The pH of the reaction mixture was adjusted to 5.8 by the addition of 0.1 M NaOH or HCl solution. The reaction was allowed to continue at room temperature for 24 hr. Then, the reaction solution was exhaustively dialyzed against deionized water followed by lyophilization. To synthesize the final product, 50mg of poly (l-glutamic acid hydrazide)-co-poly (l-glutamic acid) was dissolved in 70 ml of anhydrous methanol, and 20  $\mu$ L of trifluoro-acetic acid was added. Dox hydrochloride was then added, and the mixture was stirred at room temperature for 48 hr under nitrogen gas. Polymer Dox (pDox) was concentrated, dialyzed in methanol, and vacuum concentration.

### **Characterizations of hexagonal hematite nanodisc and donut**

The morphologies of donuts were evaluated by field emission scanning electron microscopy (FE-SEM, JSM-7000F, Japan) and transmission electron microscopy (TEM, JEM-2100, Japan). The particles were dispersed in deionized water and dried on the silicon wafer and carbon film-supported copper grids under vacuum at room temperature for specimen preparation. Dynamics laser scattering (DLS) analysis by using a particle sizer (Nano-ZS, Malvern, UK) determined the average size and size distribution of hexagonal hematite nanodisc and donut which were diluted with deionized water. Zeta-potential of particles was analyzed by Nanosizer instrument (Zetasizer Nano ZS). N<sub>2</sub> adsorption-

desorption isotherms was measured by using Autosorb 1 MP (Quantachrome Instruments, Florida, USA). BJH and BET method were respectively used to calculate pore size and surface area of the samples. Porous particles and donuts were dried at 60 °C under vacuum for 24 h, and degassed at 200 °C for 2 h before analysis. Field-dependent magnetization curves were evaluated by superconducting quantum interference device (SQUID, Quantum Design MPMS-XL7, USA) from -10,000 to 10,000 Oe at 300K. The field sensitive temperature dependence of magnetization was evaluated from 5K to 300K at 50 Oe.

### **Magnetic thermal heating of hexagonal hematite nanodisc and donut.**

High frequency magnetic field (HFMF, power cube 32/900, President Honor Industries) with a frequency of 50 kHz at a strength of 4 kA/m is applied to induce the magnetic thermal effect of different particles. The solution containing 1 mg/ml of particles was set in the coil of MF and been heated at the altitude of 70% for 10 min continuously, and the temperature were measured by a thermal couple.

### **Drug loading efficiency and release**

Dox or pDox loading porous particles (mesoporous silica, polystyrene@silica, and donut) was performed by mixing 1 % Dox or pDox with particles in de-ionic water for 12 h. Then, the mixture was placed into vacuum at 50 °C for 24 h to evaporate de-ionic water. The un-loaded Dox or pDox was then removed by PBS washing for three times. To quantify the drug loading, the drug loading efficiency (LE%) and encapsulation efficiency (EE%) of various particles contained Dox and pDox were determined by fluorescence reader (Ex. 480 nm, Em. 578 nm).  $LE(\%) = (\text{Initial Dox weight} - \text{weight of unloaded Dox}) / (\text{Weight of the particles}) \times 100\%$ .  $EE(\%) = (\text{Initial Dox weight} - \text{Weight of unloaded DOX}) / \text{Weight of the initial Dox weight} \times 100\%$ . The loading capacity was also calculated while identifying the concentration of drug.

For *in vitro* release experiment, drug-loading particles were placed in dialysis tubing and immersed in 3 mL of three kinds of different of pH value phosphate buffer solution (PBS, containing

0.1% w/v, pH 7.4, 6.7 and 5.9). At different time points, the solution was measured with a fluorescence reader (Ex. 480 nm, Em. 578 nm).

### **Cellular uptake, distribution, and cytotoxicity of donuts**

B16F10 (a murine tumor cell line; skin melanoma cells) cells were cultured in Dulbecco's modified eagle medium (DMEM) with 10 % fetal bovine serum and 1 % penicillin/streptomycin in a 5 % CO<sub>2</sub>-enriched environment at 37 °C. When the cells were incubated for 24 h, the various particles were placed to the cells for different concentrations. The cytotoxicity treated by various conditions was evaluated by a counting approach. Trypsin was applied to remove the cell from dish, and then, the cells were scored under the microscopy. The live and dead cells were counted up to 6 times and three individual experiments were evaluated for all conditions. For imaging tracking, CdSe quantum dots (QDs) were embedded in the porous particles before drug loading. In brief, the particles were added into 4 ml of n-butanol. Then, QDs were dispersed in CHCl<sub>3</sub>, and the mixture was added with the particles solution. The mixture was vortexed and sonicated for 5 min, and the particles were separated by centrifugation at 7,000 rpm. The excess of ethanol was used to washed the particles for three times. Then, the QDs-labelled particles were cultured to B16F10 cells which were grown on glass coverslips for 24 h in advance. After incubation at 37 °C for various time points, the medium was removed from the cells, which were washed twice with PBS, fixed for 30 min with 3% formaldehyde (PBS solution). Then, permeabilization was performed with 0.1% Triton X-100 (PBS solution) for 30 min and washed twice with PBS. Finally, the nuclei and actin cytoskeleton were staining with DAPI (1 µg/mL) and F-actin (300 units/mL) for 30 min, respectively. The cells were mounted on glass slides and observed by CLSM (Zeiss LSM 780).

For quantification of the cellular uptake of particles, B16F10 cells were both seeded into 6-well tissue culture plates at a density of  $1 \times 10^5$  cells per well. After incubated for 24 h, various particles labeled with quantum dots (QDs) were added in the well for different time duration respectively to observe the cell uptake. Then, the cells were washed by PBS, and then, treated with trypsin-EDTA.



The treated cells were suspended and collected with DMEM containing 10% FBS and 1% penicillin-streptomycin. The cells were centrifuged at 1,000 rpm for 10 min, and carefully collected with PBS. Next, flow cytometry (BD FACSCANTO) was used to measure the fluorescence of cells and the data were evaluated by a WinMDI 2.8 software, to quantify the amount of particle uptake by cells (accumulating 10,000 events).

### **Multicellular spheroids chip fabrication**

The multicellular spheroids chip was prepared by polydimethylsiloxane (PDMS) through soft lithography approach. Briefly, a negative photoresist (SU-8, MicroChem) was photolithographically patterned on silicon wafers to fabricate masters about 480 microwells for cell spheroids formation. The masters were then used as molds of the top cover and the bottom microchannel, on which a PDMS pre-polymer (Sylgard 184, Dow Corning) added into the crosslinking agent (10:1) with rapid mixing was then cured in a conventional oven at 65 °C for 3 h. The cured PDMS replicas were peeled off from the molds smoothly. A puncher with a 0.75 mm inner diameter was applied to form inlet and outlet holes on the top cover for the fluidic channel. The bottom microchannel was coated with poly(2-hydroxyethyl methacrylate) (pHEMA, BioReagent, powder, suitable for cell culture) which was dissolved in an ethanol solution (60 mg/mL in 95% ethanol). To improve the coating quality and cell formation efficiency, the bottom PDMS substrate was firstly oxygen plasma treatment treated to increase its hydrophilicity and then added 100 µL of pHEMA solution homogeneously. Afterward, the top cover and the bottom microchannel replicas were aligned and joined by oxygen plasma treatment, and then placed in a conventional oven at 65 °C for 24 h to achieve permanent bonding to obtain a complete multicellular spheroids chip.

### **Multicellular spheroids chip evaluation of donuts**

$5 \times 10^6$  cells/mL of B16F10 cells were loaded into the multicellular spheroids chip. For each chip, 200 µL cell solution was injected, and until the loaded cells were settled down in the microwells, 400

$\mu$ L fresh medium was applied with a high flow rate (100  $\mu$ L/min) to remove the upstream cells. After the loading process, PE lines were used to fill the inlet and outlet holes and the chip was put into 10 cm dish with some wet cotton to preserve the humidity during incubation. B16F10 spheroids were uniformly distributed inside each microwell as shown in the supporting information. After the formation of tumor spheroids, the drug-loading particles (10 $\mu$ g/mL for each nanomaterial) were infused into the chip to estimate the therapeutic efficacy by the percent of the live cell spheroids before and after MF treatment. For the tumor penetration study, the chip treated by MF or control group were estimated by CLSM (Zeiss LSM 780), where quantum dots (QDs)-labelled particles showed in red, F-actin of cells represented in green, and nucleus (DAPI) stained in blue. Before quantifying the amounts of cell viability, Live/Dead kit was applied to figure out the cell activity. Before measurement, the cells were washed by PBS for three times to remove the free particles. To investigate the MF effect of pDox@donut on MTSs, B16F10 tumor spheroids cultured with pDox@donut were subjected to MF for 5 min after 4 h of incubation, and then the pDox distribution in the spheroids was estimated after another 20 h of incubation.

### **Microfluidic chip with two channels**

The microfluidic chip with two channels was prepared with polydimethylsiloxane (PDMS) using soft lithography techniques. The negative photoresist (SU-8, MicroChem, Newton, MA, USA) for each layer was constructed on silicon wafer through photolithographically patterning. Then, sylgard 184 (Dow Corning) PDMS pre-polymer mixed with its crosslinker at a 10:1 ratio was poured and allowed to cure in a conventional oven at 60 °C for 3 h. The cured PDMS replicas were removed from the patterned substrates. The design for each layer was shown in Figure S9a. Between the center layers, the channels were separated by a collagen-coated permeable polytetrafluoroethylene (PTFE) membrane (1.4 mm x 25 mm) with 10  $\mu$ m pores. Next, with treated by oxygen plasma, the PDMS replicas and membrane were placed in an oven at 65 °C for 24 h for bonding. For cell seeding,  $2 \times 10^5$  of B16F10 or bEnd.3 cells were cultured on the membrane for 24 h to form the high density of cell

membrane. bEnd.3 cell line was a mouse cerebral micro-vascular endothelial cells (ATCC® CRL-2299™). The cells were cultured in Dulbecco's modified Eagle's medium (DMEM), containing 10% of fetal bovine serum. The other culture condition was similar to B16F10 cells. Then, various particles at a concentration of 0.2 mg/mL were injected into the chip at a constant rate of 100  $\mu$ L/min with a syringe pump for 30 min and subsequently examined by CLSM and transepithelial electrical resistance (TEER) measurement. For TEER measurement, the cells were cooled to room temperature for 20 min. Then, the TEER value of chip determined by an EVOM epithelial volttohmmeter and chopstick electrodes (World Precision Instruments).[S1]

### ***Iv vivo study***

For the animal study, all surgical procedures were performed in accordance with the protocol approved by the Institutional Animal Care and Use Committee (IACUC), National Tsing Hua University, Hsinchu, Taiwan (IACUC protocol and approval number is 10704). Female C57BL/6 mice of 6 to 8 weeks old (purchased from National Laboratory Animal Center, NLAC, Taiwan) were adopted as the animal model of tumor growth inhibition experiment. To obtain a metastatic lung cancer-bearing animal model, mice were injected with 100  $\mu$ m of  $5 \times 10^5$  of B16F10 cells using a 27-gauge needle through a tail vein. For imaging purposes, Cy<sup>®</sup>5.5 Mono NHS Ester (Cy5.5 channel, excitation: 640 nm, emission: 700 nm, Merck) was applied to label donuts in PBS solution at 37 °C. After the conjugation, the excess of Cy<sup>®</sup>5.5 Mono NHS Ester was removed by PBS washing for three times. Then, *in vivo* imaging system (IVIS Imaging System 200 Series, Caliper LifeScience, USA) was used to investigate accumulation of particles labeled with dye based on the fluorescence of Cy5.5 on the tumor sites and analyze the amounts of the different carriers in the mice.

To introduce the enhanced green fluorescent protein (EGFP)-expressing lung metastases, the mouse melanoma cell line B16F10 was purchased from Food Industry Research and Development Institute, Hsinchu and the B16F10 carrying EGFP expression vector cell line was obtained from Professor Chang CW, Department of Biomedical Engineering and Environmental Sciences, National

Tsing Hua University, Hsinchu. The cell lines were cultured in DMEM (Hyclone, SH30243) supplemented with 10% fetal bovine serum (Hyclone, SH30088). Cells were incubated at 37°C in a humidified atmosphere with 5% CO<sub>2</sub>. To obtain a GFP-metastatic lung cancer-bearing animal model, female C57BL/6 mice of 6 to 8 weeks old (purchased from National Laboratory Animal Center, NLAC, Taiwan) were injected with 100 µm of  $5 \times 10^5$  of EGFP-B16F10 cells using a 27-gauge needle through a tail vein. To track the accumulation of lung metastasis, 100 µL of pDox@donut at 2 mg/mL or PBS was injected intravenously to GFP-B16F10 lung metastasis -bearing C57B6/L mice. After 24 h, the lungs were harvested from mice and evaluated by CLSM (Zeiss LSM 780), where nuclei stained by DAPI were represented in blue, the blood vessels labeled by CD 31 were exhibited in purple and pDox@donut was represented in red.

### ***In vivo* flow cytometry analyses**

The isolated tissues were digested by 0.1 mg/mL collagenase solution (Sigma, C0130), 1 µg/mL DNase solution (Sigma, DN25), and 6.6 µg/mL dispase I solution (Sigma, D4818) in HBSS buffer (Sigma, H8264) for 90 minutes and then, fixed by 4% PFA for 30 minutes. The amount of mesoporous nanoparticles, EGFP-B16F0, endothelial cells, cytotoxic T cells, and helper T cells were analyzed by flow cytometry after the surface staining for 1 hour for primary antibody and 30 minutes for secondary antibody in the room temperature. The endothelial cells were identified using the rat-anti -CD31 antibody (BD Pharmingen, 550274, 1:200 dilution) and anti-rat-Alexa647 (Jackson, 112605167) to develop signal. The characterization of the T cell subsets was performed using fluorochrome-conjugated anti-mouse mAbs: anti-CD4 PE (BD, 553730), anti-CD3e FITC (BD, 553062), anti-CD8a APC (BD, 553035), and anti-CD45 PE-Cy7 (BD, 552848). Data were acquired using a BD FACSAria™ III flow cytometer (BD Biosciences) and analyzed with FlowJo software (Tree Star).

### **Gating strategy of flow cytometry**

To analyze the particle accumulation in tumor and endothelial cells in lung, the gating way is depended on different cell size and complexity. The cells population in flow cytometry can be divided

into 4 regions (Figure S20a). (1) Region 1 is the cell debris and erythrocytes, as the size is too small and too simple. (2) Based on the cell size, we supposed that Region 2 is lymphocytes.[S2,S3] Another staining of cells also displayed that Region 2 is composed of lymphocytes (Figure S20b). (3) According to the cell size and complexity, Region 3 represents the granulocytes.[S2,S3] (4) Due to the characteristic of endothelial cells and tumor cells, they required the enzyme to break the adherens junction to isolate the single cells. The cell size and complexity of endothelial cells and tumor cells are higher than the lymphocytes and granulocyte. Therefore, region 4 is our target to analyze. (5) CD31, a common marker to label the endothelial cells, is also expressed in lymphocytes and granulocytes.[S4-S6] To prevent false-positive results, we did not pick up all regions to conduct the analysis. The endothelial cells account for a large proportion of the lung. Therefore, we took the endothelial cells as the marker to determine the uptake of particles in the normal lung cells. This experiment can demonstrate the different uptaking rates between the normal cells and the tumor cells.

### **Immunohistochemistry (IHC) staining**

IHC staining was conducted using the protocol providing by Abcam plc. Briefly, the lungs were isolated and fixed in 4% PFA overnight and then, the tissue was embedded into optimal cutting temperature (OCT) compound (Sakura Finetek, 4583) at -80°C preparing for histologic section. After the frozen section, the samples were dehydrated and fixed in -20°C 100% methanol for 10 minutes. The fixed samples were washed by phosphate buffered saline (PBS) (Gibco, 10010023) to remove residual OCT compound. Next, the sections were incubated with the antibody solution which was diluted in 5% BSA solution at 4°C overnight with the appropriate primary antibodies, including rat-anti-CD-4 (Abcam, ab25475, 1:1000 dilution), rabbit anti-CD8 (Abcam, ab217344, 1:1000 dilution), and rat-anti-CD31 (BD Pharmingen, 550274, 1:200 dilution). The secondary antibody was then introduced into the samples at room temperature for 1 hour, which included anti-rat-Alexa647 (Jackson, 112605167) anti-rabbit-Alexa647 (Abcam, ab150075), and anti-rat-Alexa488 (Jackson, 112545143). Finally, the sections were mounted in fluoroshield mounting medium (Abcam, ab104139) and gained

the results by using the confocal microscope (Carl Zeiss, LSM800).

### **Biodistribution and survival rate with synergistic therapy *in vivo***

To evaluate the biodistribution and survival rate with synergistic chemotherapy, mice were injected with 100  $\mu\text{m}$  of  $5 \times 10^5$  of B16F10 cells using a 27-gauge needle through a tail vein to obtain a metastatic lung cancer-bearing animal model. After 6 days of tumor growth, the animals randomly grouped into four groups (n=6) were injected intravenously with 100  $\mu\text{L}$  of solution containing with particles labeled by CdSe quantum dots intravenously. Quantitative determination of Cd in each organs and tumors by ICP-MS. The survival rates of all groups were recorded every day from the day of B16F10 cells implantation (n=6).


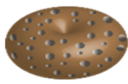
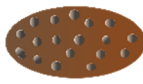
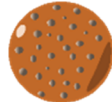

### **Results and Discussion**

For PGA, the characteristic absorption band in the IR spectrum at  $1610\text{ cm}^{-1}$  was attributed to the stretching vibration of C=O groups. Furthermore, two peaks at 1530 and  $1489\text{ cm}^{-1}$  were ascribed to amide I and II bands, respectively. Modified PGA was also investigated via monitoring the new peaks at  $1637$  and  $1432\text{ cm}^{-1}$ , revealing the superposition of C=O vibrations and the amide I and II groups both in PGA and ADH (Figure S4). Representative  $^1\text{H}$  NMR spectra of PGA-ADH-Dox, PGA, and EDC and ADH are presented in Figure S5. The degree of PGA-ADH modification was determined from the relative peak areas of the peaks at 1.56 and 4.22 ppm, corresponding to the methylene protons (4H,  $\text{CH}_2\text{-CH}_2$ ) of ADH and the protons binding to the  $\alpha$ -carbon of L-glutamic acid. Then, pDox molecules were loaded

into the porous discoidal donut, and the physicochemical characteristics and loading efficiency of pDox are summarized in Table S2.

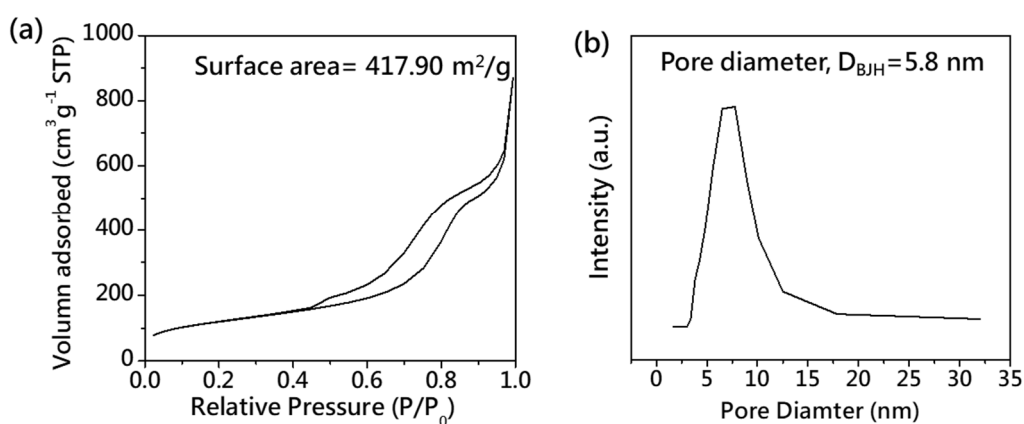
Concerning toxicity, liver function, such as alanine aminotransferase (ALT) and alkaline phosphatase (ALP) levels, were estimated 72 h after administration (Figure 5g). Compared to the control group, the higher toxicity of pDox treatment was detected, whereas pDox@donut exhibited a negligible difference, revealing the low toxicity of pDox@donut. Furthermore, the kidney function, as measured by blood urea nitrogen (BUN) and serum creatinine (CRE), of pDox and pDox@donut displayed higher values than that of control, indicating a slight toxicity of these therapeutic agents for the kidney.

**Table 1.** Synthesis of various particles by controlling TEOS and styrene concentration.

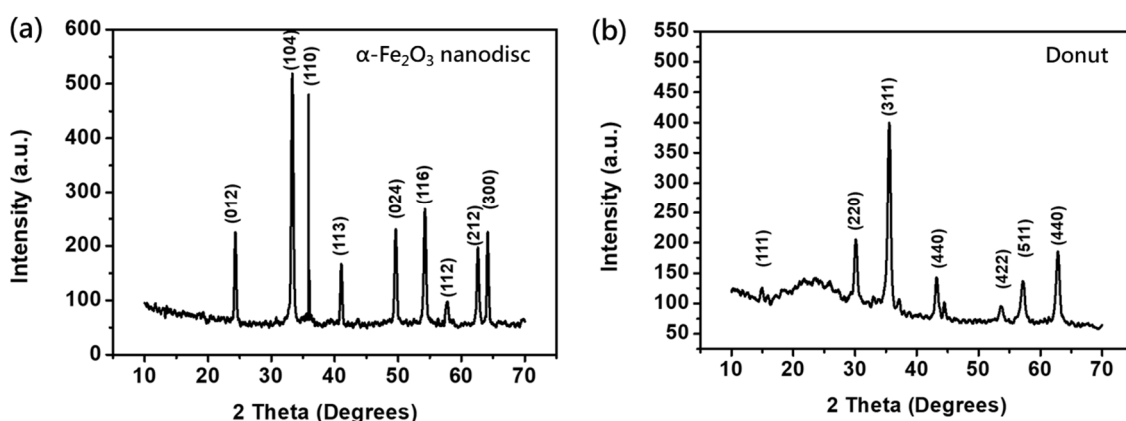
	Sun-like disc	Donut	Ellipse	Sphere	Rod
					
substrate	$\alpha$ -Fe <sub>2</sub> O <sub>3</sub> nanodisc	$\alpha$ -Fe <sub>2</sub> O <sub>3</sub> nanodisc	$\alpha$ -Fe <sub>2</sub> O <sub>3</sub> nanodisc	None	$\alpha$ -Fe <sub>2</sub> O <sub>3</sub> nanorod
n-octane	14.4 mL	14.4 mL	14.4 mL	14.4 mL	14.4 mL
styrene	5 mg/mL	20 mg/mL	50 mg/mL	100 mg/mL	50 mg/mL
TEOS	0.24 mmol	0.94 mmol	2.35 mmol	4.7 mmol	2.35 mmol
lysine	0.146 mmol	0.146 mmol	0.146 mmol	0.146 mmol	0.146 mmol

**Table 2.** Physicochemical characterization of pDox and pDox@donut. The loading efficiency of pDox to donut.

Identity	Result	Measurement
pDox NP size (pH 7.4)	0.5-2 nm	DLS
pDox NP zeta potential (pH 7.4)	-0.0131 mv	Zetasizer
Percentage Dox in pDox	13%	Fluorescence
Percentage pDox NP in donut (w/w)	19%	Fluorescence
Encapsulation efficiency (E.E.%)	55%	Fluorescence
Size of release pDox from donut (pH 7.4)	80~100 nm	DLS
Size of release pDox from donut (pH 6.7)	50~70 nm	DLS
Size of release pDox from donut (pH 5.9)	50~70 nm	DLS

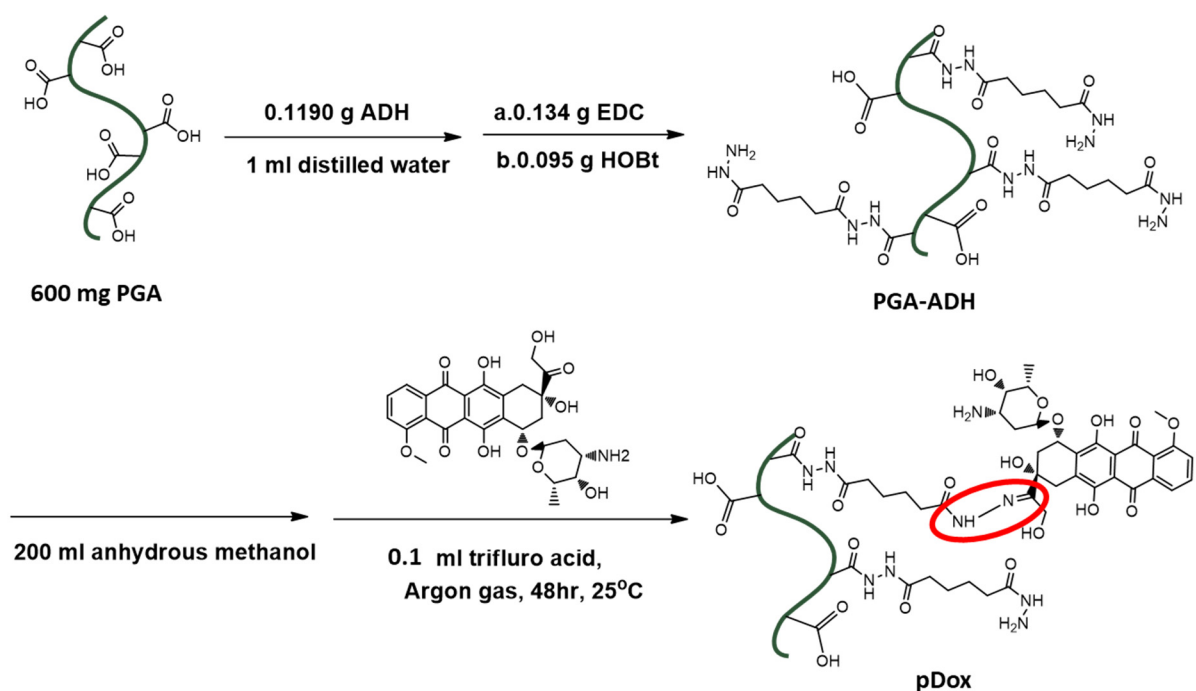


**Figure S1.** (a) N<sub>2</sub> adsorption–desorption isotherms of donuts. (b) Pore diameter distribution of donuts based on Barrett-Joyner-Halenda (BJH) analysis.

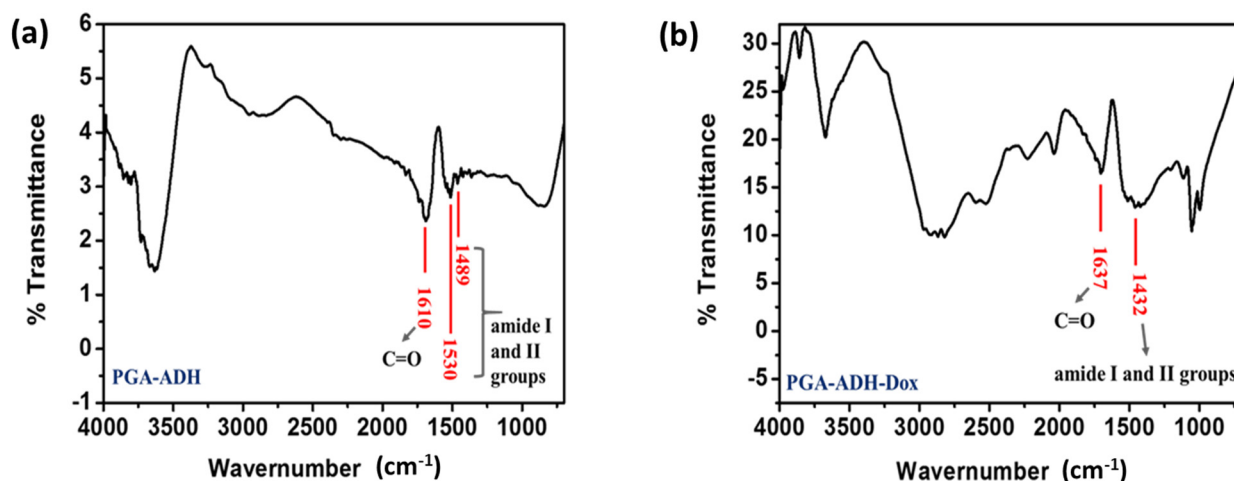


**Figure S2.** X-ray diffraction patterns of (a) as-synthesized hexagonal hematite (α-Fe<sub>2</sub>O<sub>3</sub>) nanodiscs and (b) donuts (Fe<sub>3</sub>O<sub>4</sub>, JCPDS [85-1436]).



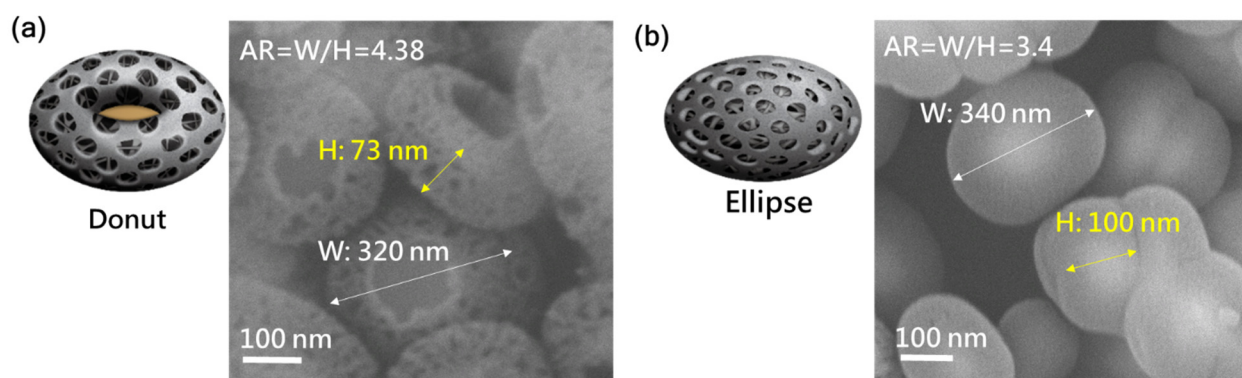


**Figure S3.** Synthesis of poly Dox (pDox). 1-Ethyl-3-(3- (dimethylaminopropyl) carbodiimide hydrochloride (EDC) were used as the carboxylic acid activators to proceed the reaction between poly ( $\gamma$ -glutamic acid) (PGA) and adipic acid dihydrazide (ADH). Chemical structure of the pDox prodrug is shown, and the pH-sensitive hydrazone linker is circled in red.

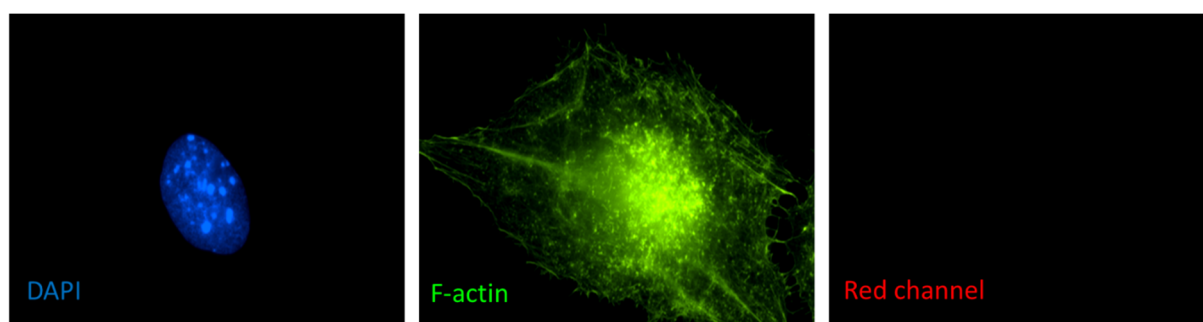


**Figure S4.** FTIR spectra of (a) PGA-ADH and (b)  $\gamma$ -PGA-ADH-Dox (pDox).

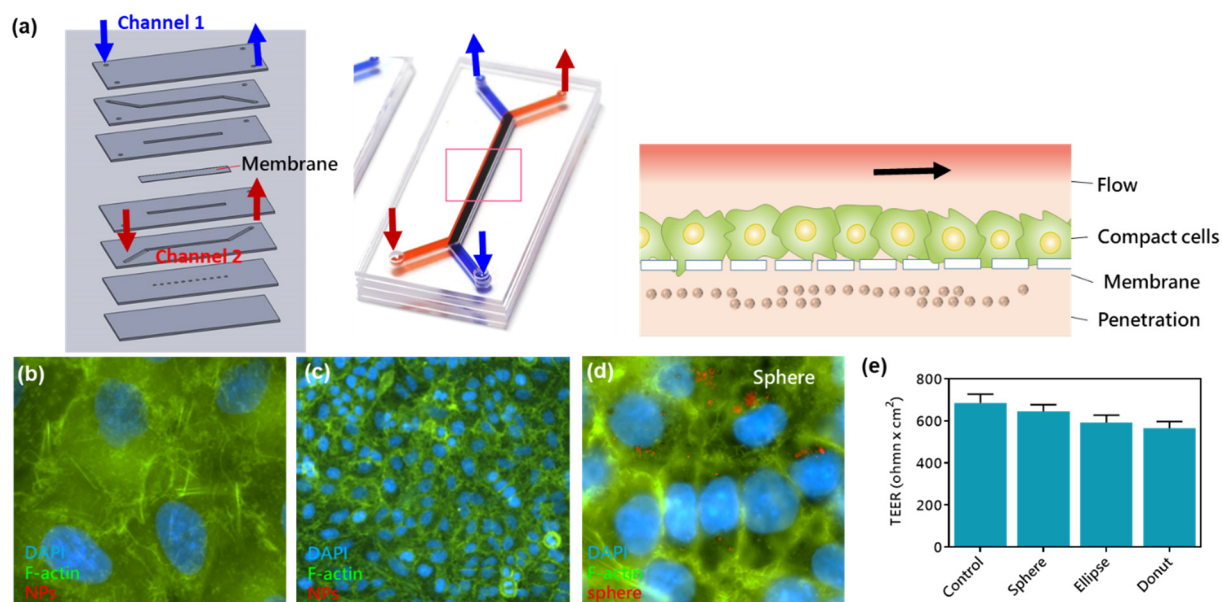




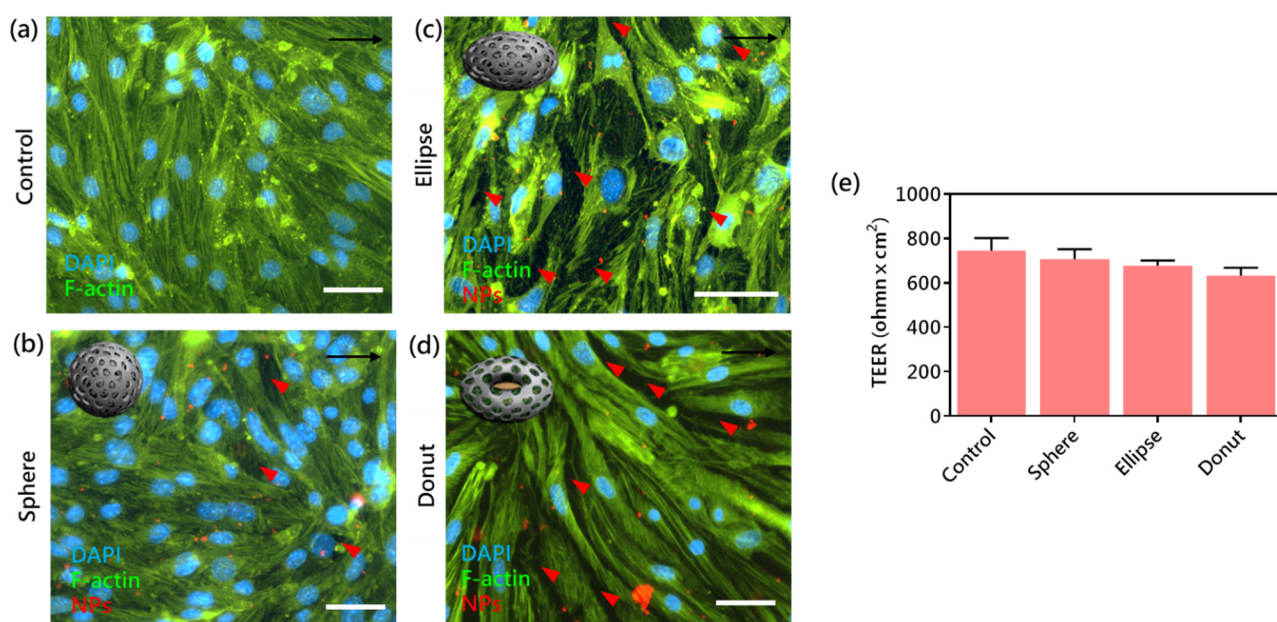
**Figure S7.** The aspect ratios of (a) donut and (b) ellipse, estimated by SEM images.



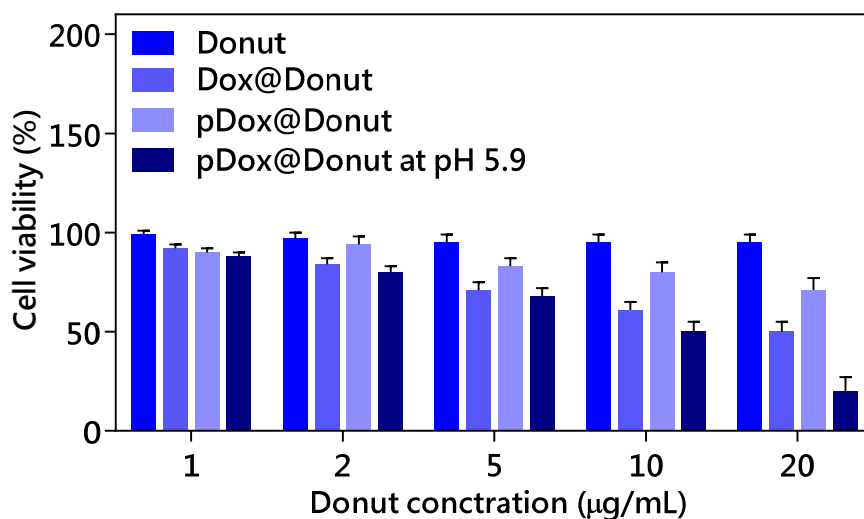
**Figure S8.** Control experiment on A549 cells without treating by any particle.



**Figure S9.** (a) A microfluidic chip with two channels separated by a collagen-coated permeable polytetrafluoroethylene (PTFE) membrane with 10  $\mu\text{m}$  pores for formation of a cell sheet. (b,c) CLSM images of a cell sheet in a chip at 24 h postinjection. (d) The accumulation of spheres on a chip investigated by CLSM. (e) TEER measurements of B16F10 cells after treated by various particles (n = 6).

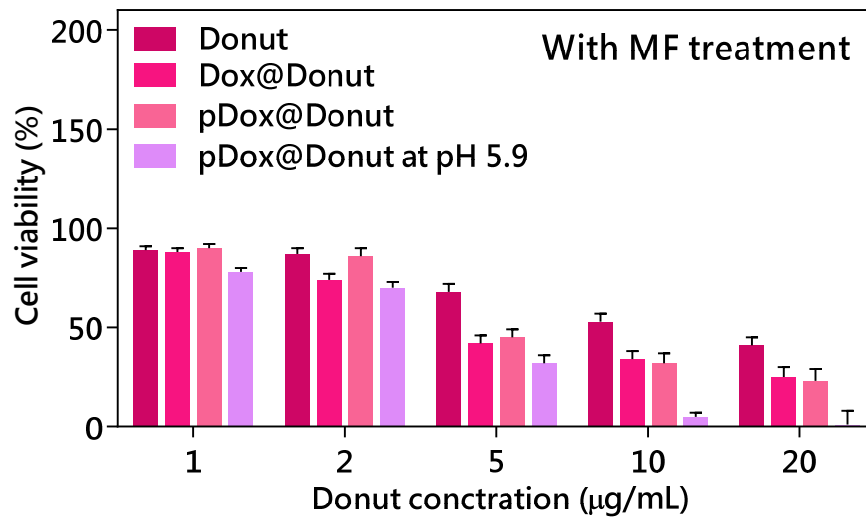


**Figure S10.** bEnd.3 cell line, a mouse cerebral micro-vascular endothelial cells, was seeded on a microfluidic chip with two channels separated by a collagen-coated permeable PTFE membrane to form a cell sheet. (a) CLSM images of a cell sheet in a chip at 24 h postinjection. (b-c) The CLSM images of cell sheet treated by spheres, ellipse and donuts. Amounts of ellipses or donuts attached on the cell sheets through the margination effect, and the leakages between the cells were found. (e) TEER measurements of bEnd.3 cells after treated by various particles (n = 6).

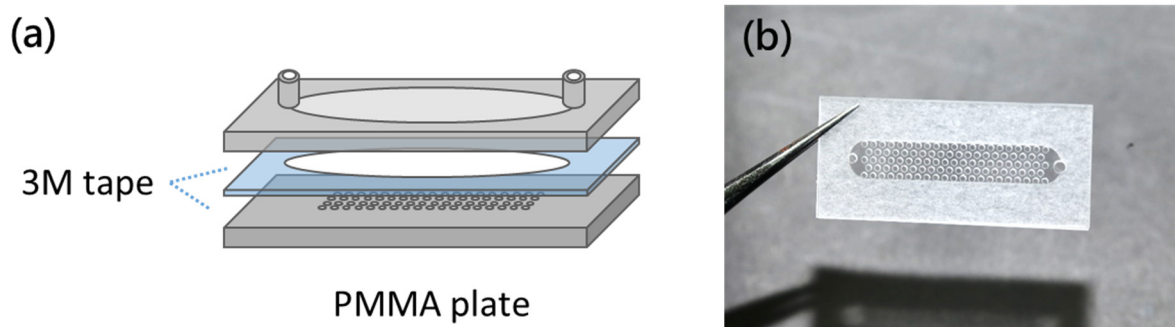


**Figure S11.** Cell viability after incubating with B16F10 cells for 24 h with donut, Dox@donut and pDox@donut at various concentrations.

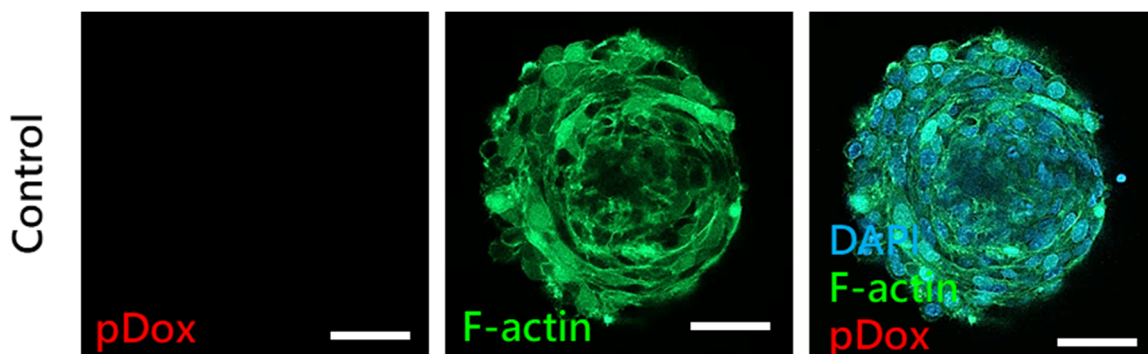




**Figure S12.** Cell viability after incubating with B16F10 cells for 24 h with donut, Dox@donut and pDox@donut at various concentrations. At the fourth hour, B16F10 cells cultured were subjected to MF for 5 min.



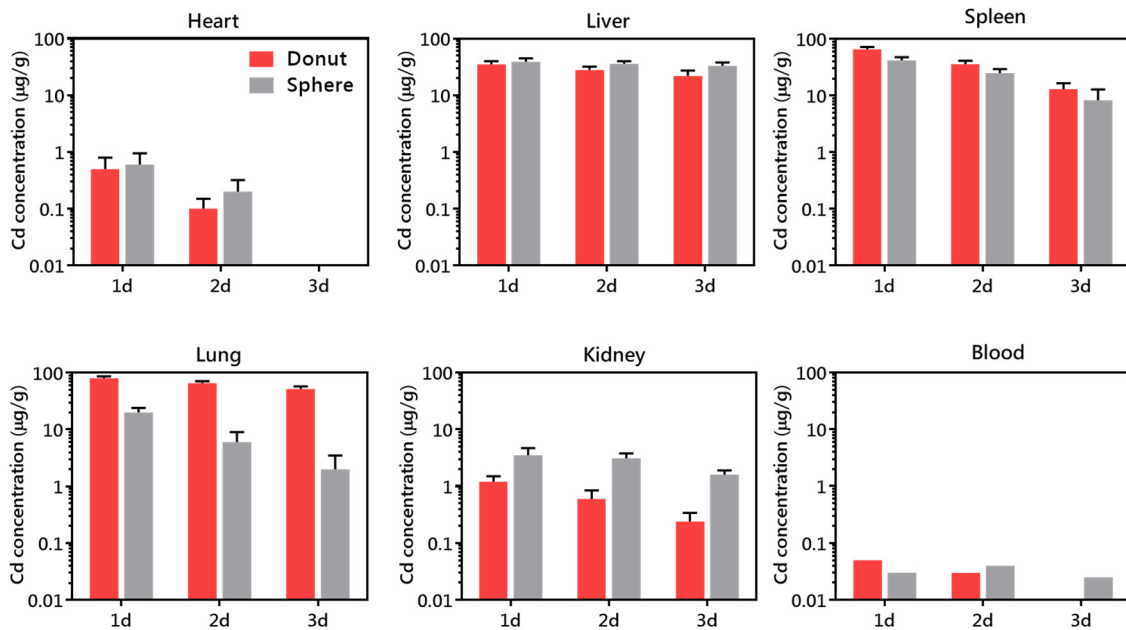
**Figure S13.** MTSs chip was built through a microfluidic chip-based approach for high-throughput formation and long-term culture of tumor spheroids. (a) The design of a microfluidic chip. (b) The picture of MTSs chip.



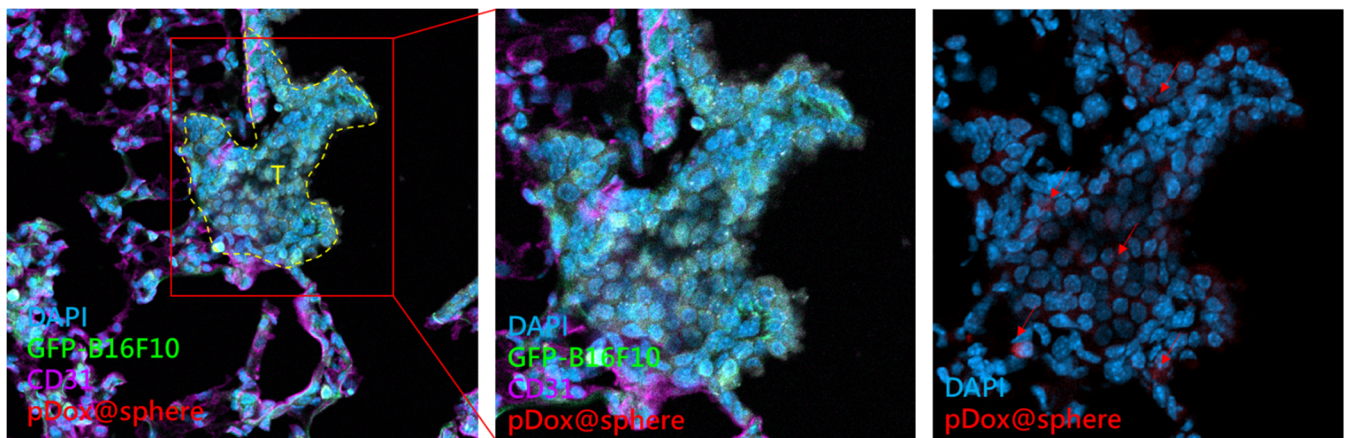
**Figure S14.** CLSM images of tumor spheroids on a chip after 1 day of incubation.



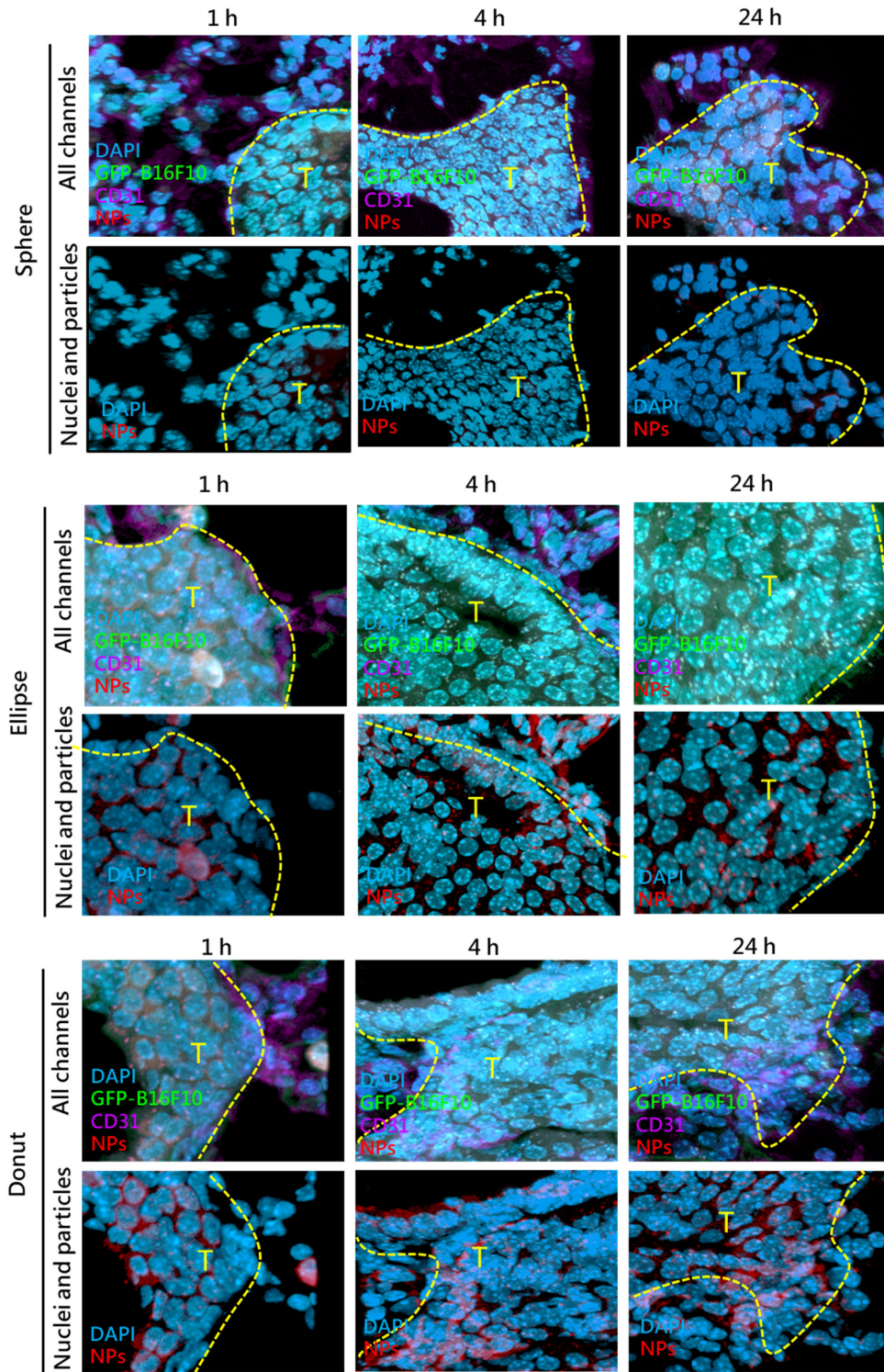
**Figure S15.** (Left) The normal lung. (Right) The formation of numerous metastatic foci in lung at 14 days postinjection of GFP-B16F10 cells.



**Figure S16.** The organ accumulation of donut and sphere at 24, 48 and 72 h postinjection (n=5).

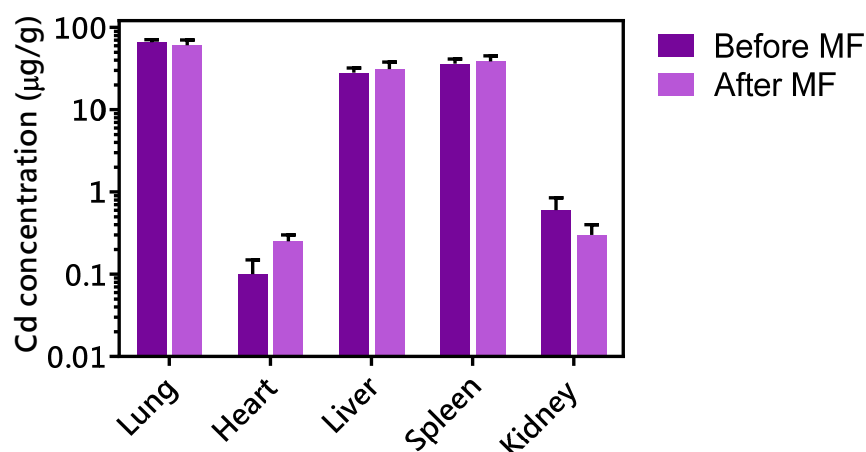


**Figure S17.** CLSM images of lung metastases treated by pDox@sphere. The lung metastases were displayed in green (GFP-B16F10 cells), nuclei were represented in blue, the blood vessels labeled by CD 31 were exhibited in purple and pDox@sphere was represented in red.

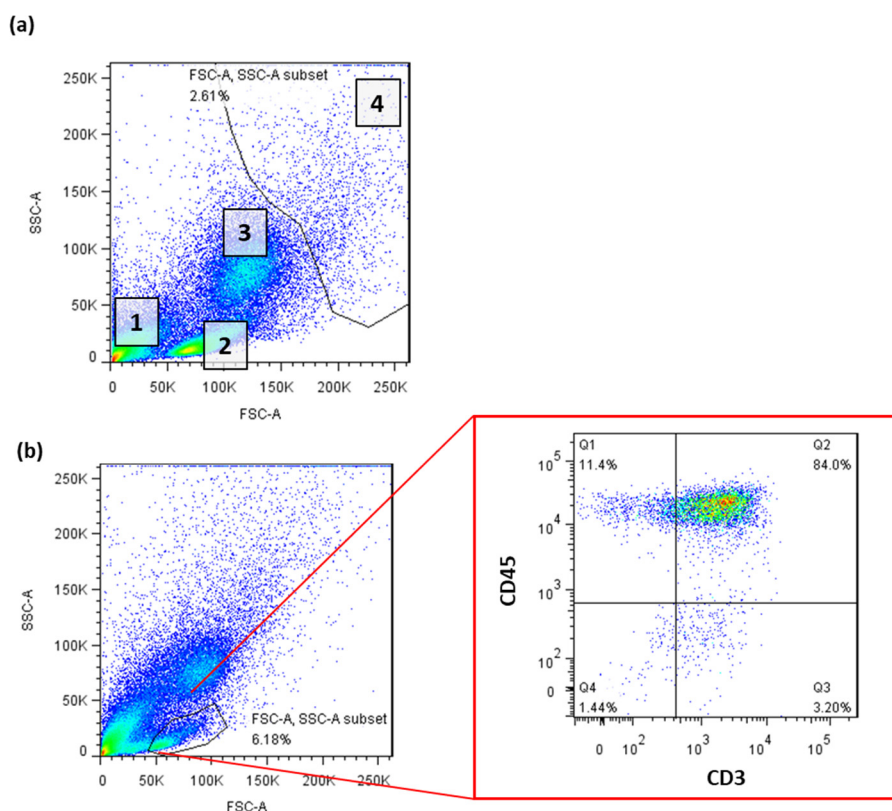


**Figure S18.** CLSM images of lung metastasis-bearing mice at 1, 4, and 24 h postinjection of (a) donut, (b) sphere and (c) ellipse. The lung metastases are displayed in green and the blood vessels labeled by CD 31 are exhibited in purple. At 1 h postinjection of donut- and ellipse- like particles, the lung metastasis revealed the relatively clear fluorescence signal when compared to sphere particles. With increasing time, the accumulation of various-shaped particles was enhanced, and the donuts showed the strongest fluorescence on the lung metastasis.



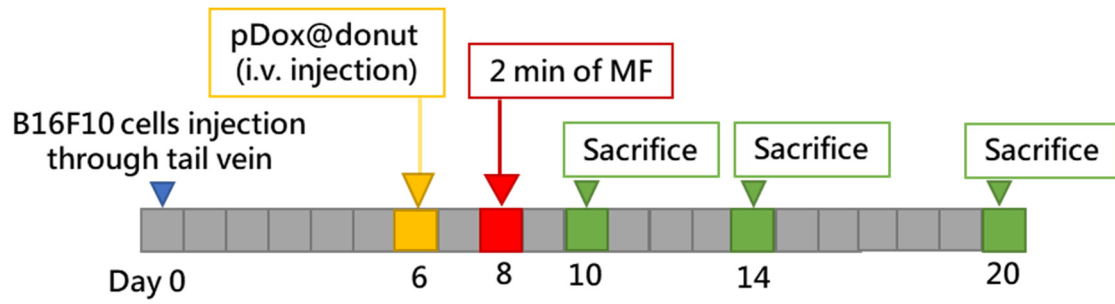


**Figure S19.** The biodistribution of the donuts before and after MF treatment by the quantitative determination of Cd in each organ by ICP-MS. Briefly, 100 µL of donuts labelled by CdSe QDs was injected into C57B6/L mice bearing lung metastases. At 24 h of postinjection, the mice treated with and without MF for 2 min were sacrificed at 4 h of posttreatment (n=5).

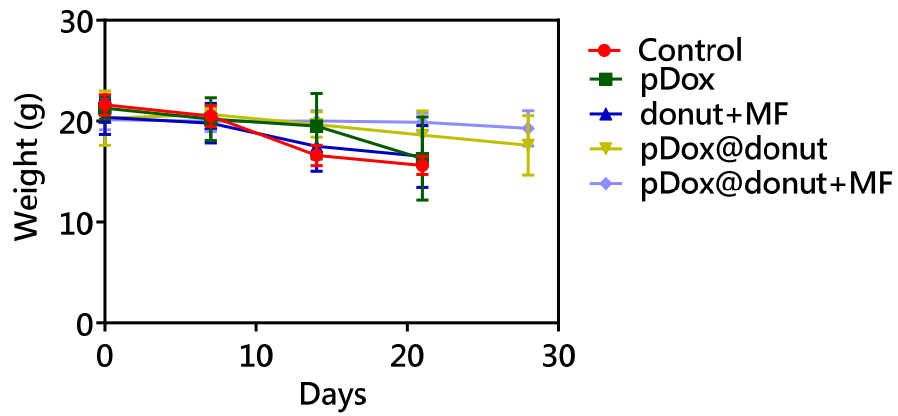


**Figure S20.** (a) Gating strategy of tumor cells and endothelial cells in flow cytometry. (b) Flow cytometry analysis of the cells labeled with anti-CD3 and anti-CD45 antibodies.

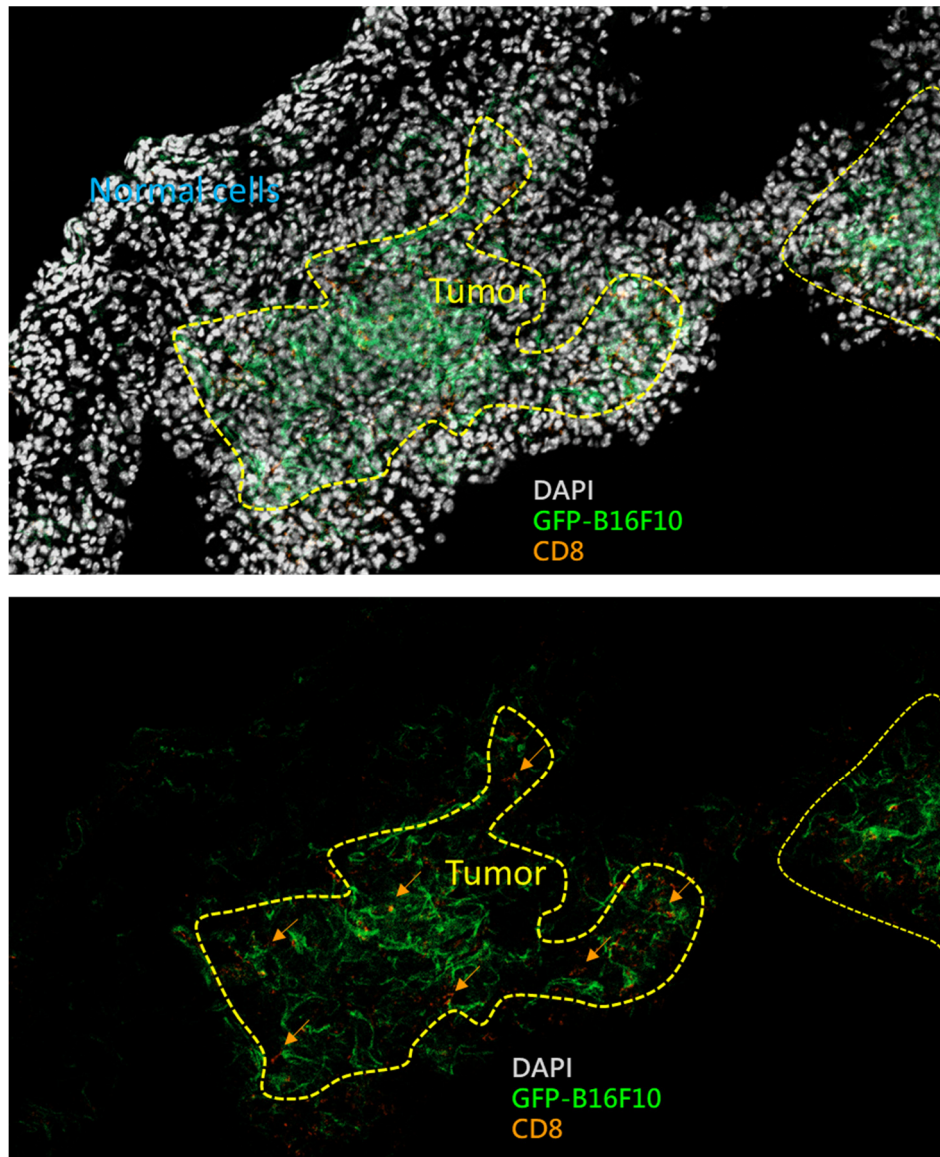




**Figure S21.** The animal study schedule of treating C57B6/L mice-bearing GFP-B16F10 lung.



**Figure S22.** Mice weights of B16F10 lung metastases-bearing mice after treated with PBS (control), pDox, donut+MF, pDox@donut and pDox@donut+MF (n=6).



**Figure S23.** CLSM images of a lung of mouse treated by pDox@donut with MF, where the lung sections labeled with anti-CD8 antibodies.

- [S1] B. Srinivasan, A. R. Kolli, M. B. Esch, H. E. Abaci, M. L. Shuler, J. J. Hickman, TEER measurement techniques for *in vitro* barrier model systems. *J. Lab Autom.*, **2015**, 20, 107.
- [S2] L. K. Ashman, G. W. Aylett, Expression of CD31 epitopes on human lymphocytes: CD31 monoclonal antibodies differentiate between naive ( $CD45RA^+$ ) and memory ( $CD45RA^-$ ) CD4-positive T cells, *Tissue Antigens*, **1991**, 38, 208.
- [S3] D. J. Cavatorta, H. N. Erb, M. J. Felipe, Activation-induced FoxP3 expression regulates cytokine production in conventional T cells stimulated with autologous dendritic cells, *Clin. Vaccine Immunol.*, **2012**, 19, 1583.
- [S4] A. J. Fike, L. T. Nguyen, O. K. Kumova, A. J. Carey, Characterization of CD31 expression on murine and human neonatal T lymphocytes during development and activation, *Pediatr. Res.*, **2017**,

82, 133.

- [S5] K. Kawabata, S. Nakai, M. Miwa, T. Sugiura, Y. Otsuka, T. Shinzato, N. Hiki, I. Tomimatsu, Y. Ushida, F. Hosono, and K. Maeda, CD31 expression on leukocytes is downregulated *in vivo* during hemodialysis, *Nephron*, **2001**, 89, 153.
- [S6] P. Lertkiatmongkol, D. Liao, H. Mei, Y. Hu, P. J. Newman. Endothelial functions of platelet/endothelial cell adhesion molecule-1 (CD31), *Curr. Opin. Hematol.*, **2016**, 23, 253.